Roles for Cyclopentenyl Cations in the Synthesis of Hydrocarbons from Methanol on Zeolite Catalyst HZSM-5

James F. Haw,[*,†] **John B. Nicholas,**[*,‡] **Weiguo Song,**[†] **Feng Deng,**[†] **Zhike Wang,**[§] **Teng Xu,**[§] **and Catherine S. Heneghan**[†]

Contribution from the Loker Hydrocarbon Research Institute and Department of Chemistry, University of Southern California, University Park, Los Angeles, California 90089-1661, Environmental Molecular Sciences Laboratory, Pacific Northwest National Laboratory, P.O. Box 999, Richland, Washington 99352, and Department of Chemistry, Texas A&M University, P.O. Box 300012, College Station, Texas 77842-3012

Received November 23, 1999

Abstract: In situ ^{13}C NMR measurements on samples prepared using a pulse-quench catalytic reactor show that the 1,3-dimethylcyclopentenyl carbenium ion (**1**) is an intermediate in the synthesis of toluene from ethylene on zeolite catalyst HZSM-5. Cation **1** forms in less than 0.5 s when ethylene is pulsed onto the catalyst bed at 623 K, and its presence obviates the kinetic induction period for conversion of a subsequent pulse of dimethyl ether, or methanol, into olefins (MTO chemistry). The kinetic induction period returns when the interval between pulses is many times the half-life of **1** in the catalyst bed. Density functional theory calculations (B3LYP/6-311G**) on a cluster model of the zeolite confirm that **1** is stable in the zeolite as a free cation and suggest why the alternative framework alkoxy is not observed. A π complex of the neutral cyclic diene is only 2.2 kcal/mol higher in energy than that of the ion pair. Theoretical (GIAO-MP2/tzp) ^{13}C isotropic shifts of isolated **1** are in good agreement with the experimental spectra of the cation in the zeolite. To understand how organic species entrained in the catalyst could promote MTO chemistry, we calculated a number of methylation reactions in the gas phase. We found that the diene formed by deprotonation of **1** is far more easily methylated than ethylene, propene, or toluene. The aggregate experimental and theoretical results reveal the essential features of a mechanism for MTO and methanol to gasoline (MTG) chemistry on a working catalyst.

Methanol-to-gasoline (MTG) chemistry[1,2] on zeolite HZSM-5 has motivated more fundamental study[3] than any other mechanistic problem in heterogeneous catalysis. There is also much current interest in the closely related process of methanol-to-olefin (MTO) chemistry, which is also catalyzed by HZSM-5 using different process conditions[4] to minimize aromatic formation. Dehydration of methanol to dimethyl ether (DME) is rapid, and identical hydrocarbon distributions are obtained with either oxygenate. From a fundamental perspective, MTG and MTO processes on HZSM-5 pose the same mechanistic questions: *On a working catalyst*, how is methanol (or DME) converted into olefins, why is propene formed with higher initial selectivity than other olefins, and, how are aromatics synthesized under MTO/MTG conditions?

MTG/MTO chemistry has been intensely studied using theoretical methods,[5−11] infrared spectroscopy,[12,13] and NMR.[14−21]

At least 20 distinct mechanisms have been proposed for the first carbon−carbon bond-forming step, and most of these predict that ethylene is the first hydrocarbon product. It is usually assumed that propene and other higher olefins arise by homologation of ethylene with methanol or dimethyl ether (DME). However, a key feature of the reaction is a kinetic induction period that precedes large-scale hydrocarbon synthesis, and the reaction occurring during the induction period need not be the same as that on a working catalyst. Several workers have applied classical flow-reactor methods to the study of the induction period. In a previous series of papers that is very pertinent to the present investigation, Kolboe studied the effect of prior introduction of olefin precursors on the subsequent conversion of methanol.[22−25] He found that treated catalysts were more

† University of Southern California.

‡ Pacific Northwest National Laboratory.

§ Texas A&M University.

(1) Chang, C. D.; Silvestri, A. J. *J. Catal.* **1977**, *47*, 249−259.

(2) Chang, C. D. *Catal. Rev. Sci. Eng.* **1983**, *25*, 1−118.

(3) Stöcker, M. *Microporous Mesoporous Mater.* **1999**, *29*, 3−48.

(4) Kei, F. J. *Microporous Mesoporous Mater.* **1999**, *29*, 49−66.

(5) Haase, F.; Sauer, J. *J. Am. Chem. Soc.* **1995**, *117*, 3780−3789.

(6) Blaszkowski, S. R.; van Santen, R. A. *J. Am. Chem. Soc.* **1996**, *118*, 5152−5153.

(7) Blaszkowski, S. R.; van Santen, R. A. *J. Am. Chem. Soc.* **1997**, *119*, 5020−5027.

(8) Blaszkowski, S. R.; van Santen, R. A. *J. Phys. Chem. B* **1997**, *101*, 2292−2305.

(9) Tajima, N.; Tsunda, T.; Toyama, F.; Hirao, K. *J. Am. Chem. Soc.* **1998**, *120*, 8222−8229.

(10) Stich, I.; Gale, J. D.; Terakura, K.; Payne, M. C. *J. Am. Chem. Soc.* **1999**, *121*, 3292−3302.

(11) Hutchings, G. J.; Watson, G. W.; Willock, D. J. *Microporous Mesoporous Mater.* **1999**, *29*, 67−77.

(12) Forester, T. R.; Howe, R. F. *J. Am. Chem. Soc.* **1987**, *109*, 5076−5082.

(13) Campbell, S. M.; Jiang, X.-Z.; Howe, R. F. *Microporous Mesoporous Mater.* **1999**, *29*, 91−108.

(14) Anderson, M. W.; Klinowski, J. *Nature* **1989**, *339*, 200−203.

(15) Anderson, M. W.; Sulikowski, B.; Barrie, P. J.; Klinowski. *J. Phys. Chem.* **1990**, *94*, 2730−2734.

(16) Munson, E. J.; Lazo, N. D.; Moellenhoff, M. E.; Haw, J. F. *J. Am. Chem. Soc.* **1991**, *113*, 2783−2786.

(17) Munson, E. J.; Haw, J. F. *J. Am. Chem. Soc.* **1991**, *113*, 6303−6305.

(18) Munson, E. J.; Khier, A. A.; Lazo, N. D.; Haw, J. F. *J. Phys. Chem.* **1992**, *96*, 7740−7746.

(19) Hunger, M.; Horvath, T. *J. Am. Chem. Soc.* **1996**, *118*, 12302−12308.

(20) Ernst, H.; Freude, D.; Mildner, T. *Chem. Phys. Lett.* **1994**, *229*, 291−296.

(21) Goguen, P. W.; Xu, T.; Barich, D. H.; Skloss, T. W.; Song, W.; Wang, Z.; Nicholas, J. B.; Haw, J. F. *J. Am. Chem. Soc.* **1998**, *120*, 2651−2652.

active than untreated catalysts and proposed a phenomenological "carbon-pool" model to account for reactions on working catalysts. Kolboe did not attempt to characterize the structure of the carbon pool species, but he speculated that it might be a carbenium ion. In another series of investigations, Mole and co-workers demonstrated that simple aromatic hydrocarbons functioned as "cocatalysts" for methanol conversion.[26,27] They proposed a mechanism by which *exo*-methylene species, in equilibrium with protonated methyl aromatics (e.g., benzenium cations), undergo electrophilic addition to form ethylbenzenes which eliminate ethylene in acidic media. An alternative mechanism involving well-established six- to five-membered ring interconversions was also proposed to account for the findings of Mole et al.[28]

Here we report extensive experimental work using a pulse-quench catalytic reactor[21,29–31] to probe the transition between induction reactions and hydrocarbon synthesis on a working catalyst. NMR characterization of quenched catalyst samples, in combination with theoretical calculations,[32] reveals that formation of the 1,3-dimethylcyclopentenyl carbenium ion (**1**)
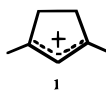
on the zeolite ends the induction period for MTO chemistry. The active site for hydrocarbon synthesis on a working catalyst is a composite of cyclic organic species, on which carbon–carbon bonds are made and broken in a catalytic cycle, and one or more Brønsted acid sites. We find that **1** is synthesized in less than 0.5 s with high selectivity when ethylene is pulsed onto the zeolite at 623 K. Variable-temperature MAS NMR experiments reveal that **1** is present on a sealed catalyst sample at 523 K. We measured the half-life of **1** in the catalyst bed in the presence of carrier gas flow and obtained values of 10 min at 548 K and 6 s at ca. 723 K. In the absence of **1**, olefin synthesis from DME exhibits a clear kinetic induction period. If **1** is first synthesized in the zeolite from natural abundance ethylene, olefin synthesis from DME-$^{13}C_2$ proceeds without an induction period, and ^{13}C labels are incorporated uniformly into **1**. The induction period returns if the time interval between injection of ethylene and DME is greater than several times the half-life of **1**. We also show that **1** is an intermediate in the synthesis of toluene, an important product in MTG chemistry.

Theoretical chemistry was used to further clarify several aspects of the experimental work. We explored the mechanism by which isolated cation **1** is converted to toluene by calculating the relative energies (MP2/6-311+G*) of various possible species that might exist on the reaction pathway. We optimized the gas-phase geometry of **1** and calculated the ^{13}C chemical shift tensors using the gauge-including atomic orbital (GIAO)

method at the MP2 level. The predicted isotopic ^{13}C chemical shifts are in good agreement with those measured for **1** in the zeolite. Density functional theory (DFT) optimizations at the B3LYP/6-311G** level confirmed that **1** forms a stable ion pair complex with a large cluster model of the HZSM-5 conjugate base site. We also found a stable neutral π complex of the cyclic diene **2** formed by deprotonation of **1** and the Brønsted site of the catalyst that was only 2.2 kcal/mol higher in energy than the ion pair. A third species, a framework alkoxy produced by forming a covalent bond between **1** and an oxygen on the conjugate base site of the catalyst, is also a stable point on the potential energy surface, but the relative energy of this species is so high as to suggest no role in the observed chemistry.
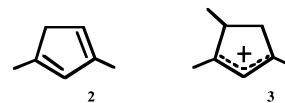
Finally, theoretical chemistry was also applied to understand how formation of **1**, **2**, and related species could end the kinetic induction period and catalyze hydrocarbon synthesis. We calculated the reaction pathways for a number of methylation reactions in the gas phase. For example, methylation of ethylene or propene with trimethyloxonium to yield protonated DME and propene or 1-butene, respectively, has predicted barriers greater than 45 kcal/mol. In contrast, methylation of cyclic diene **2** with trimethyloxonium formed DME and carbenium ion **3** with a barrier of only 33 kcal/mol. The aggregate experimental and theoretical evidence led to a proposed catalytic cycle for MTO chemistry on HZSM-5 that also accounts for propene selectivity. Similar schemes can also be constructed for alkylation and olefin elimination from aromatics as a parallel or competing pathway once these are formed from cyclopentenyl cations.

Experimental Section

Materials and Reagents. All results reported were obtained on a zeolite HZSM-5 catalyst with a Si/Al ratio of 14 that was pressed into pellets (10 to 20 mesh) without binder. Some of the experiments were repeated using a zeolite with a Si/Al of 19 as pellets with 30 wt % alumina binder. No obvious differences were observed for the two materials studied. Ethylene-$^{13}C_2$ (99% ^{13}C), propene-1-^{13}C (99% ^{13}C), propene-2-^{13}C (99% ^{13}C), and 2-methylpropene-2-^{13}C (99% ^{13}C) were obtained from Cambridge Isotopes. Dimethyl ether (DME)-$^{13}C_2$ (99% ^{13}C) was obtained from Isotec.

Catalysis Experiments. We used a pulse-quench reactor to study hydrocarbon synthesis reactions. For each experiment we loaded the reactor with a cylindrical bed (7.5 mm diameter by 8 mm in length, typical weight of 0.3 g) of fresh catalyst pellets. In every case, the catalyst bed was activated in place immediately prior to use by heating at 573 K for 1 h in flowing helium. DME pulses were 0.46 mol per mole of acid site (typically 0.15 mmol), and ethylene pulses were 1.9 mol per mole of acid site (typically 0.63 mmol). The pulse-quench reactor is essentially a fixed bed, microflow reactor. Helium (600 sccm) was used as the carrier gas, and reactants were introduced in pulses using injection valves as in refs 21, 29, and 30. Schematics of a pulse-quench reactor in a single-pulse configuration can be found in Figure 1 of ref 29. The double-pulse experiments were of the following type: Pulse 1, τ_1; Pulse 2, τ_2, quench. Pulse 1 was the first compound delivered to the catalyst bed, usually ethylene, and the treated catalyst was allowed to age for time τ_1 prior to delivery of a second reagent, frequently DME or methanol, in Pulse 2. Further aging of the catalyst occurs during the time interval τ_2. Following τ_2 the catalyst bed temperature is rapidly decreased to ambient using a thermal quench. Previous studies have shown that the temperature of the catalyst pellets decreases 150 K in the first 170 ms of a quench. In some cases we used N_2 as one of the reagents for control experiments that precisely matched other double-pulse experiments. Single-pulse experiments were

(22) Kolboe, S. *Acta Chem. Scand.* **1986**, *A-40*, 711–713.

(23) Dahl, I. M.; Kolboe, S. *J. Catal.* **1994**, *149*, 458–464.

(24) Dahl, I. M.; Kolboe, S. *J. Catal.* **1996**, *161*, 304–309.

(25) Kolboe, S. In *Methane Conversion*; Bibby, D. M., Chang, C. D., Howe, R. F.,d Yurchak, S., Eds.; Elsevier Science Publishers: Amsterdam, 1988; pp 189–193.

(26) Mole, T.; Whiteside, J. A.; Seddon, D. *J. Catal.* **1983**, *82*, 261–266.

(27) Mole, T.; Bett, G.; Seddon, D. *J. Catal.* **1983**, *84*, 435–445.

(28) Pines, H. *J. Catal.* **1985**, *93*, 205–206.

(29) Haw, J. F.; Goguen, P. W.; Xu, T.; Skloss, T. W.; Song, W.; Wang, Z. *Angew. Chem.* **1998**, *37*, 948–949.

(30) Xu, T.; Barich, D. H.; Goguen, P. W.; Song, W.; Wang, Z.; Nicholas, J. B.; Haw, J. F. *J. Am. Chem. Soc.* **1998**, *120*, 4025–4026.

(31) Barich, D. H.; Xu, T.; Song, W.; Wang, Z.; Deng, F.; Haw, J. F. *J. Phys. Chem. B* **1998**, *102*, 7163–7168.

(32) Haw, J. F.; Nicholas, J. B.; Xu, T.; Beck, L. W.; Ferguson, D. B. *Acc. Chem. Res.* **1996**, *29*, 259–267.
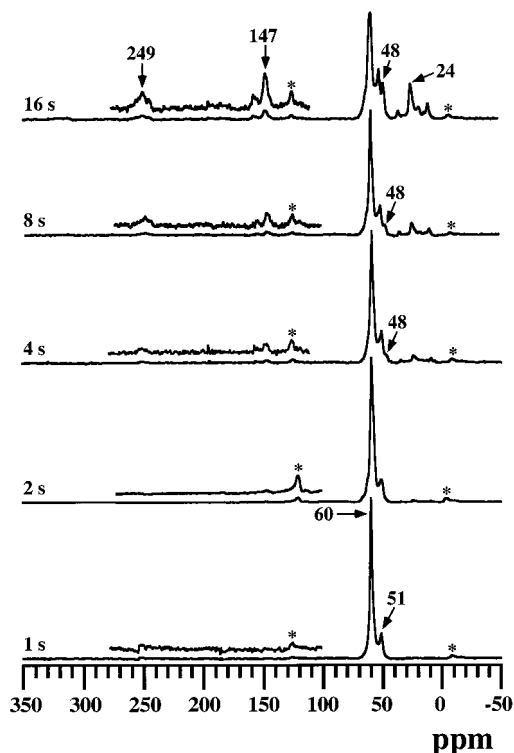
Figure 1. 75.4 MHz ^{13}C CP/MAS NMR spectra of the reaction products of dimethyl ether-^{13}C$_2$ (DME) retained on zeolite HZSM-5 following various times at 573 K in a pulse-quench reactor. In each case, 7.2 mg of DME, corresponding to ca. 0.46 molecules of DME per acid site, was injected onto a freshly activated, previously unused catalyst bed. Signals due to DME (60 ppm), a trace of methanol (51 ppm), and cation **1** are highlighted. All spectra were measured at 298 K. The asterisks denote spinning sidebands.

of the following type: Pulse 1, τ_1, quench. In both double-pulse and single-pulse experiments the gas stream exiting the reactor was sampled for gas chromatographic or GC-MS analysis. After each reacted catalyst sample was quenched, the reactor was sealed off and transferred into a glovebox filled with nitrogen (0.3 ppm of H$_2$O). The catalyst pellets were ground and transferred to a 7.5-mm MAS rotor that was sealed with a Kel-F end-cap. This procedure affords a sealed sample for MAS NMR study that has not been exposed to atmospheric moisture.

NMR Spectroscopy. ^{13}C solid-state NMR experiments were performed with magic angle spinning (MAS) on a modified Chemagnetics CMX-300 MHz spectrometer operating at 75.4 MHz for ^{13}C. Hexamethylbenzene (17.4 ppm) was used as an external chemical shift standard, and all ^{13}C chemical shifts are reported relative to TMS. Chemagnetics-style pencil probes spun 7.5 mm zirconia rotors at typically 6.5 kHz with active spin speed control ($\pm$3 Hz).

Typical ^{13}C experiments included the following: cross polarization (CP, contact time = 2 ms, pulse delay = 1 s, 2000 to 16000 transients); cross polarization with interrupted decoupling (contact time = 2 ms, pulse delay = 1 s, 2000 to 16000 transients, dipolar dephasing time of 50 μs); and single-pulse excitation with proton decoupling (Bloch decay, pulse delay = 10 s, 400 to 4000 transients). All the spectra shown were obtained with cross polarization, except where otherwise stated.

Quantitation of Cation 1 in Catalyst Samples. The absolute yields of cation **1** in several catalyst samples prepared using the pulse-quench reactor were determined by both spin counting and elemental analysis. A calibration of ^{13}C NMR signal intensity vs carbon content was obtained for measurements of five samples of hexamethylbenzene (natural abundance) in sulfur. All ^{13}C NMR spectra for spin counting experiments were measured using Bloch decays with 10 s pulse delays. The number of ^{13}C spins corresponding to one or more of the prominent signals of **1** in the catalyst samples was deduced by comparison to the standard curve. This measurement was then used to calculate the number of **1** cations per unit measure of zeolite. For several samples, con-

firmatory evidence was obtained by carbon analysis (Galbraith). Spin counting and elemental analysis results were in good agreement.

Theoretical Methods

Several different types of theoretical methods were employed in this investigation. We first needed to verify the identity of the cyclopentenyl species **1**. To this end we optimized the geometry of **1** using second-order Møller−Plesset theory (MP2) and the 6-311+G* basis set.[33] The core electrons not included in the correlation treatment. Chemical shieldings for **1** were then calculated using the GIAO method at the MP2 level.[34] We used Ahlrich's tzp basis set[35] {51111/311/1} (with 6 Cartesian d orbitals) on the carbon and dz {31} on the hydrogens in the chemical shift calculations. We term this level of theory GIAO-MP2/tzp/dz.

The calculated chemical shielding tensors were symmetrized and then diagonalized to yield principal components. These were then referenced to the ^{13}C isotropic chemical shift of carbon in tetramethylsilane (TMS) calculated at the same level of theory (for both the shielding and geometry) such that $\delta_{calc} = \sigma_{TMS} - \sigma_{calc}$. The absolute shieldings of ^{13}C in TMS is (in ppm) 199.0 at MP2/tzp/dz//MP2/6-311+G*. The isotropic chemical shift is the average of the principal components, which are defined such that $\delta_{11} \ge \delta_{22} \ge \delta_{33}$. Thus,

$$\delta_{iso} = {}^1\!/_3(\delta_{11} + \delta_{22} + \delta_{33})$$

The asymmetry factor (η) and chemical shift anisotropy (CSA) are defined as previously in ref 36.

It is also important to theoretically verify if **1** can exist as a stable cation in the presence of the conjugate base of the zeolite acid site. To this end we optimized **1** complexed to a model of a deprotonated zeolite acid site in HZSM-5. Specifically, HZSM-5 was modeled as a cluster of stoichiometry [(H$_3$SiO)$_3$SiOAl(OSiH$_3$)$_3$]$^-$. Due to the large size of the system we were unable to use the MP2 method for the geometry optimization. We thus used DFT, which provides geometries and energies comparable to MP2 calculations at a considerably reduced computational cost. For the DFT optimizations we used the hybrid B3LYP exchange-correlation functional[37] and the 6-311G** basis set. In all the optimizations the terminal silyl (H$_3$Si−) groups were held fixed in crystallographic positions corresponding to the T(12)−O(24)−T(12) site in HZSM-5.[38] The positions of all other atoms were allowed complete freedom. The constraints imposed in the optimizations impart errors in the calculated thermodynamic properties; we thus report only changes in energy (ΔE) rather than enthalpy. We also identified two additional adsorption complexes.

We used theoretical methods to explore the mechanism for conversion of **1** to toluene. Each of the possible reaction intermediates was first optimized at the B3LYP/6-311G* level of theory. Frequency calculations were done to verify that each optimized geometry was a true energy minimum (no negative eigenvalues). The B3LYP/6-311G* geometries and force constants were then used as input to MP2/6-311+G* optimizations.

Finally we calculated at the B3LYP/6-311G* level the reaction pathways for the methylation of various species as well as for elimination reactions leading to olefin products. All the optimizations and frequency calculations were done with Gaussian 94.[39] Chemical shift tensors were calculated with the program ACES II.[40]

Experimental Results

In the pulse-quench studies reported here, the NMR spectra were measured at room temperature, and each spectrum corre-

(33) Hehre, W. J.; Radom, L.; Schleyer, P. v. R.; Pople, J. A. *Ab Initio Molecular Orbital Theory*; John Wiley & Sons: New York, 1986.
(34) Gauss, J. *Chem. Phys. Lett.* **1992**, *191*, 614−620.
(35) Schafer, A.; Horn, H.; Ahlrichs, R. *J. Chem. Phys.* **1992**, *97*, 2571−2577.
(36) Barich, D. H.; Nicholas, J. B.; Xu, T.; Haw, J. F. *J. Am. Chem. Soc.* **1998**, *120*, 12342−12350.
(37) Becke, A. D. *J. Chem. Phys.* **1993**, *98*, 5648−5652.
(38) van Koningsveld, H.; van Bekkum, H.; Jansen, J. C. *Acta Crystallogr.* **1987**, *B43*, 127−132.

sponds to a unique catalyst sample. Catalyst samples were discarded after a single use, and all experiments began with freshly activated catalyst. In this investigation, catalyst samples have "histories" only within a given double-pulse experiment, when Pulse 1 could influence the outcome of reactions following Pulse 2.

Single-Pulse Experiments. We previously used a pulse-quench reactor to observe the induction period in the conversion of methanol to hydrocarbons on zeolite HZSM-5.[21] The first step in that reaction, equilibration of methanol with DME and water, is exothermic and not relevant to the mechanism of hydrocarbon synthesis. For this investigation we used DME as the starting material to avoid this preequilibrium. Figure 1 presents ^{13}C MAS NMR spectra from a pulse-quench study of the reactions of DME-$^{13}C_2$ on HZSM-5 catalyst pellets. DME (60 ppm) does not react at all on fresh catalyst for the first 2 s at 573 K; between 4 and 8 s there is a very modest conversion to form small amounts of cation **1** (peaks assigned below), after which large scale hydrocarbon synthesis commences. GC or GC-MS analysis of the hydrocarbon products exiting the reactor invariably show a preponderance of propene relative to other olefins and, in particular, high propene-to-ethylene ratios. High selectivity for propene has previously been observed.[41] The results in Figure 1 are consistent with the kinetic induction period well-known to MTG chemistry. By similar experiments, we determined that the induction period for DME on HZSM-5 was ≥ 16 s at 548 K and ca. 0.5 s at 623 K.

We used the pulse-quench reactor to study the reactions of ethylene-$^{13}C_2$ on the catalyst. The heats of adsorption and reaction of ethylene are significant and must be considered in evaluating the reaction temperature. The pulse-quench reactor was equipped with a high-speed (5 ms) thermocouple that was placed in contact with the catalyst pellets 4 mm from the front of the catalyst bed. Under steady-state reaction conditions the temperature of the catalyst bed is well regulated; this is not possible during high concentration pulses of reactive species. Thermocouple traces for three experiments in which 0.63 mmol of ethylene was pulsed onto catalyst beds at various temperatures are reported in the Supporting Information (Figure S1). Briefly, the arrival of the ethylene pulse onto the catalyst pellets is heralded by a ca. 100 K temperature increase which persists for several seconds. We also found that 0.15 mmol DME pulses resulted in ca. 20 K temperature transients. In the following we distinguish between the temperature of the catalyst bed prior to (or several seconds after) an ethylene pulse and a transient temperature ca. 100 K higher immediately following an ethylene pulse, whenever the distinction may be important.

Figure 2 reports ^{13}C MAS NMR results for single-pulse experiments in which ethylene was exposed to the catalyst at an initial temperature of 623 K (the temperature during the first few seconds of reaction rose to ca. 723 K) and allowed to react between 0.5 and 16 s prior to quenching. The most prominent peaks in the spectrum obtained for 0.5 s of reaction are all due to **1**. These are the isotropic resonances at 250 ppm, C1 and
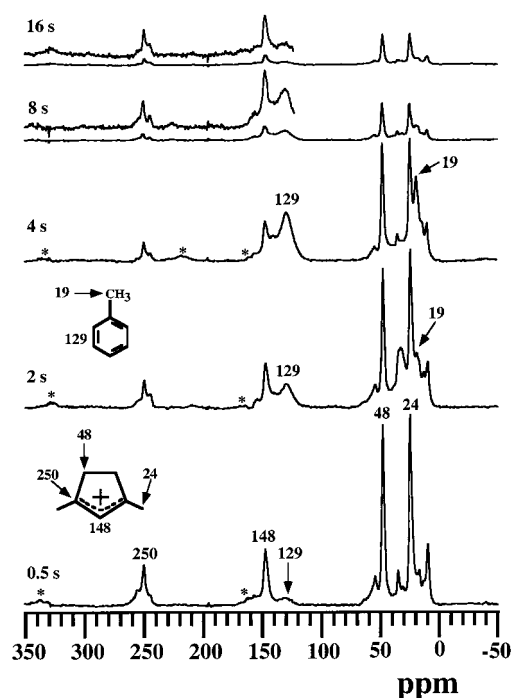
(39) Frisch, M. J.; Trucks, G. W.; Schlegal, H. B.; Gill, P. M. W.; Johnson, B. G.; Robb, M. A.; Cheeseman, J. R.; Keith, T.; Petersson, G. A.; Montgomery, J. A.; Raghavachari, K.; Al-Laham, M. A.; Zakrzewski, V. G.; Ortiz, J. V.; Foresman, J. B.; Cioslowski, J.; Stefanov, B. B.; Nanayakkara, A.; Challacombe, M.; Peng, C. Y.; Ayala, P. Y.; Chen, W.; Wong, M. W.; Andres, J. L.; Replogle, E. S.; Gomperts, R.; Martin, R. L.; Fox, D. J.; Binkley, J. S.; Defrees, D. J.; Baker, J.; Stewart, J. P.; Head-Gordon, M.; Gonzalez, C.; Pople, J. A. *Gaussian 94, Revision B.2*; Gaussian, Inc.: Pittsburgh, PA, 1995.
(40) ACES II, an ab initio quantum chemical program system; Stanton, J. F.; Gauss, J.; Watts, J. D.; Lauderdale, W. J.; Bartlett, R. J.
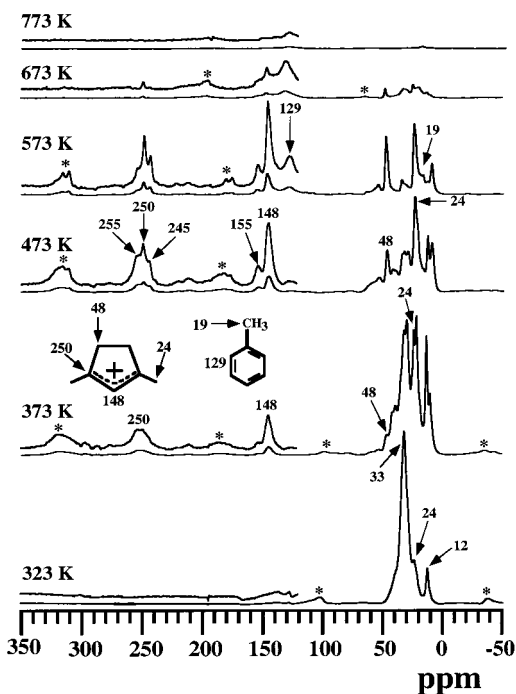(41) Chu, C. T-W.; Chang, C. D. *J. Catal.* **1984**, *86*, 297−300.

Figure 2. ^{13}C CP/MAS NMR spectra of the reaction products of ethylene-$^{13}C_2$ retained on zeolite HZSM-5 following various times at 623 K in a pulse-quench reactor. Signals from cyclopentenyl cations (250, 148, 48, and 24 ppm) and toluene (129 and 19 ppm) are indicated in the spectra. All spectra were measured at 298 K. The asterisks denote spinning sidebands.

C3 of the allyl cationic moiety; 148 ppm, C2 of the allyl cationic moiety; 48 ppm, CH_2 carbons; and 24 ppm, CH_3 carbons. These assignments were verified by interrupted decoupling (also called dipolar dephasing) experiments. They are also consistent with previous studies of cation **1** in acidic solutions and our theoretical studies (vide infra). As the catalyst ages for 2 to 4 s, signals due to **1** decrease with a commensurate increase in signals due to toluene at 129 and 19 ppm. With further aging in the flow reactor, signals due to toluene and other organics diminish, and after 16 s only a modest amount of **1** remains in the catalyst bed. A semilog fit of the decrease of **1** over time yielded an approximate half-life of 6 s. We carried out an analogous experiment at a nominal temperature of 548 K and found that the half-life of cation **1** in the catalyst bed was ca. 10 min at the lower temperature. The latter results are presented in the Supporting Information (Figure S2).

Figure 3 reports a series of ethylene single-pulse experiments in which the reaction time was fixed at 4 s, but the initial reaction temperature was varied between 323 and 773 K. A remarkable reaction occurred at the lowest temperature studied, 323 K. The ^{13}C NMR spectrum of this sample is reminiscent of those of long-chain alkanes. Interrupted decoupling experiments established that the 12 ppm signal was the only one due to methyl groups in this sample. The 33 ppm signal is consistent with CH_2 groups well removed from chain ends and the 24 ppm signal is characteristic of methylenes immediately adjacent to chain ends. This spectrum is due to unbranched oligomers of ethylene, and if no cyclic species are present, integration suggests an average chain length of up to 40 carbons. When similar experiments were conducted at higher temperatures, the unbranched oligomers were replaced with more complex products including cation **1** and closely related species. For example, the peak at 155 ppm has previously been assigned to the C2 carbons in cations with substitution patterns similar to

Synthesis of Hydrocarbons

J. Am. Chem. Soc., Vol. 122, No. 19, 2000 4767

Figure 3. ^{13}C CP/MAS NMR spectra of the reaction products of ethylene-^{13}C$_2$ retained on zeolite HZSM-5 following 4 s of reaction at various temperatures (indicated) in a pulse-quench reactor. Toluene (129 and 19 ppm) is one of the products formed from **1** at higher temperatures. All spectra were measured at 298 K. The asterisks denote spinning sidebands.

4.[42] We also verified this assignment by theoretical calculations

4
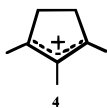
(vide infra). At least three isotropic peaks are partly resolved in the 245−255 ppm range for samples prepared at initial temperatures of 473 or 573 K; this is further evidence of cyclopentenyl cations with diverse substitution patterns. Accumulation of toluene in the catalyst bed is apparent for the reaction carried out at an initial temperature of 573 K. Essentially no organic species were retained on the catalyst bed after 4 s of reaction at 773 K.

GC traces from the experiments which also provided the NMR spectra shown in Figure 3 are collected in Figure 4. Some of the ethylene passes through the reactor without conversion to other products. For samples prepared at intermediate temperatures (473−573 K) for which **1** and related cations were apparent in the NMR spectra, the corresponding GC traces are dominated by C$_4$ and C$_5$ products in approximately equal amounts. The high yield of C$_5$ compounds is clearly inconsistent with formation of primary products by a simple oligomerization of ethylene. At higher temperatures (e.g., 773 K) the products are dominated by propene and aromatics, *most prominently toluene*, with smaller amounts of benzene and xylenes. Again, the high yield of an odd-carbon product, toluene, is significant.

We discovered that the formation of **1** and similar cations in flow reactors is a general characteristic of simple olefins. Single-pulse experiments were performed in which propene (two isotopomers) and 2-methylpropene were reacted for 4 s at 623 K. In every case aromatics were also formed and label
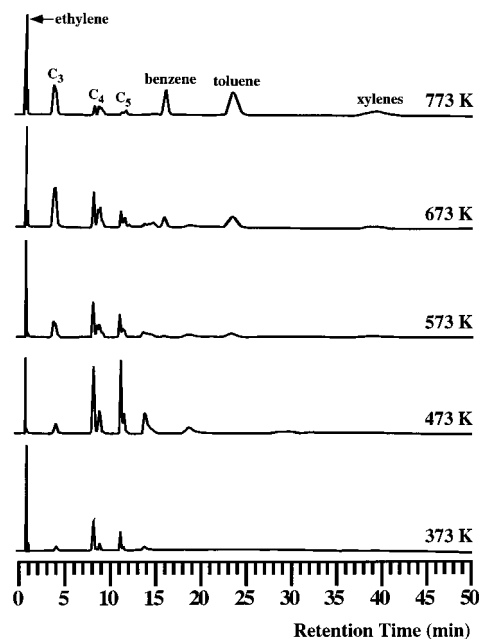
(42) Haw, J. F.; Richardson, B. R.; Oshiro, I. S.; Lazo, N. L.; Speed, J. A. *J. Am. Chem. Soc.* **1989**, *111*, 2052−2058.

Figure 4. GC traces (thermal conductivity) characterizing the volatile products from the reactions of ethylene-^{13}C$_2$ on zeolite HZSM-5 (4 s reaction time) at various temperatures in a pulse-quench reactor. Toluene is a major product at higher temperatures.

scrambling in the cations appeared to be quantitative. ^{13}C NMR spectra from these studies are included as Figure S3 in the Supporting Information; they are similar in appearance to those from analogous experiments using ethylene-^{13}C$_2$.

We used NMR spin counting and elemental analysis to measure the absolute yields of cation **1** in experiments representative of those reported here. In particular, we studied samples prepared by pulsing ethylene-^{13}C$_2$ onto catalyst samples at 623 K followed by reaction between 0.5 and 60 s. Spin counting and elemental analysis results were consistent; the yields of **1** were only 1−4% of all acid sites, corresponding to absolute yields of up to one cation per ca. four unit cells or one cation per ca. 16 channel intersections. This yield is low enough that we might expect to see mass transport in the catalyst little affected by formation of **1**. Using standard vacuum line techniques, we measured benzene uptakes for both fresh catalysts and catalysts reacted to form **1** and found them indistinguishable.

Double-Pulse Experiments. Double-pulse experiments established that the formation of **1** by prior injection of ethylene had a profound effect on the subsequent reaction of DME. Figure 5 reports experiments carried out at 548 K, a temperature at which the induction period is much greater than 8 s and the half-life of **1** in the catalyst is 10 min. Without prior injection of ethylene (Figure 5a) there is negligible conversion of labeled DME after 8 s. Figure 5b reports a result obtained by injecting a pulse of natural abundance ethylene, waiting 60 s, injecting labeled DME, allowing a further 8 s of reaction, then quenching. In this case there was significant conversion of DME as measured by hydrocarbon products in the GC trace, the diminished DME peak in the NMR spectrum, and the appearance of ^{13}C labels in peaks for cation **1**. Figure 5c is a control experiment which establishes that **1** derived from ethylene in the first pulse is still present in the catalyst bed 68 s later. Ethylene-^{13}C$_2$ was injected followed 60 s later by a pulse of N$_2$; 8 s later the sample was quenched. Signals due to **1**, related cations, and some toluene are readily apparent in the spectrum. We carried out analogous experiments in which the catalyst was allowed to age up to 10 min after injection of ethylene and prior
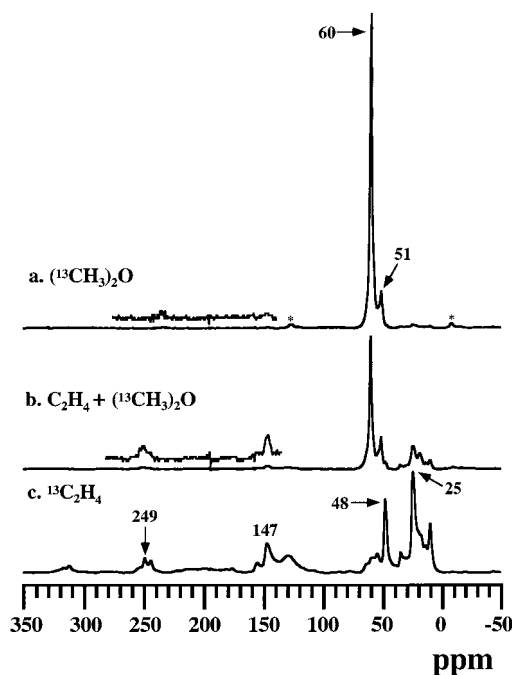
Figure 5. ^{13}C CP/MAS NMR studies of the reactions of DME-[13]C_2 with cyclopentenyl cations at 548 K on zeolite HZSM-5 in a pulse quench reactor. Spectrum a corresponds to the reaction of DME-[13]C_2 for 8 s on zeolite HZSM-5, showing almost no hydrocarbon formation. Spectrum b corresponds to a double pulse experiment; ethylene (natural abundance) was first injected and reacted for 60 s on zeolite HZSM-5 to form cyclopentenyl cations, then DME-[13]C_2 was injected and reacted for 8 s. The yields of hydrocarbons, including cation **1**, are much higher in the second experiment. Spectrum c corresponds to a double pulse control experiment; ethylene-[13]C_2 was first injected and reacted for 60 s, then N_2 was injected and the catalyst was quenched after a further 8 s. The control experiment demonstrates that cation **1**, formed from the injection of ethylene, is present on the catalyst long enough to influence the conversion of DME 68 s later.

Figure 6. ^{13}C CP/MAS NMR studies of the reactions of DME-[13]C_2 with cyclopentenyl cations at 573 K on zeolite HZSM-5 in a pulse quench reactor. Spectrum a corresponds to the reaction of DME-[13]C_2 for 8 s on zeolite HZSM-5, showing almost no hydrocarbon formation. Spectrum b corresponds to a double pulse experiment; ethylene (natural abundance) was first injected and reacted for 60 s on zeolite HZSM-5 to form cyclopentenyl cations, then DME-[13]C_2 was injected and reacted for 8 s. The yields of hydrocarbons, including cation **1**, are much higher in the second experiment. Spectrum c corresponds to a double pulse control experiment; ethylene-[13]C_2 was first injected and reacted for 60 s, then N_2 was injected and the catalyst was quenched after a further 8 s. The control experiment demonstrates that cation **1**, formed from the injection of ethylene, is present on the catalyst long enough to influence the conversion of DME 68 s later.

to injection of DME, and still observed that the induction period for hydrocarbon synthesis from DME was eliminated by the presence of **1**. Very significantly, when we allowed the catalyst bed to age for 180 min (many times the half-life of **1**) the induction period for reaction of DME returned as if ethylene had never been injected. This experiment (Figure S4, Supporting Information) strongly supports the role of **1** and related species in hydrocarbon synthesis on working catalysts in that removal of the proposed cause eliminates the observed effect.

Figure 6 reports an analogous set of experiments at a higher reaction temperature, 573 K. After 8 s of reaction in a single-pulse experiment, DME was still within the induction period on fresh catalyst, although traces of **1** had begun to form (Figure 6a). When a larger amount of **1** was preformed by injecting natural abundance ethylene and allowing the catalyst to age for 60 s, the subsequent conversion of labeled DME after 8 s of reaction was greatly enhanced (Figure 6b), and ^{13}C labels from DME were incorporated into **1**. In similar double-pulse experiments we observed some conversion of DME with τ_2 as short as 0.5 s. Figure 6c reports a control experiment demonstrating that **1** is indeed present in the catalyst 68 s after injection of ethylene-[13]C_2.

Stability of Cation 1 in the Catalyst. Most of the in situ NMR studies carried out in our laboratory in the past decade have reacted adsorbates on catalysts in sealed rotors heated or cooled in variable-temperature MAS NMR probes.[43] While this experimental approach does not simulate flow reactors or permit
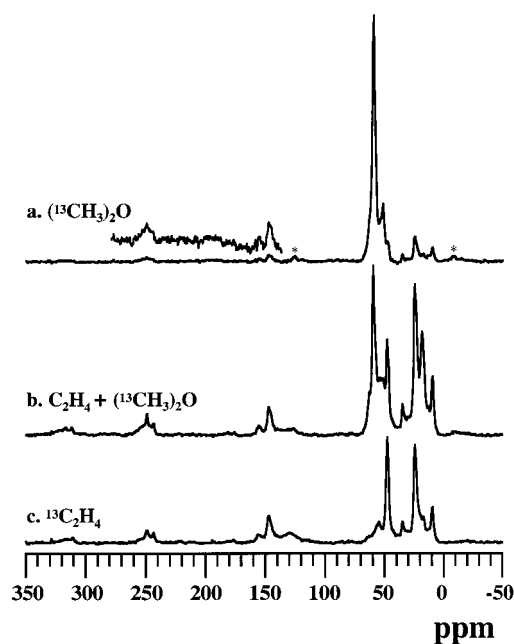
studies to be carried out at short reaction time scales, it has one advantage in that the NMR measurement can be made at higher temperatures, sometimes approaching those in a catalytic reactor. Since the pulse-quench reactor prepares samples at high temperatures for NMR measurements at room temperature, we considered the possibility that **1** is not present at high temperature but is the *reversible* reaction product of other species (e.g., olefins) trapped in the catalyst by the thermal quench. We used the pulse-quench reactor to prepare catalyst samples loaded primarily with **1** (formed from ethylene-[13]C_2), sealed these in MAS rotors, and then carried out conventional variable-temperature in situ studies. A representative result is reported in Figure 7. These studies show that **1** is stable on the zeolite in a sealed rotor up to at least 523 K; we observed some conversion to toluene, but most of the **1** was unreacted after prolonged heating. The resonances of **1** were slightly broader at 523 K compared to those at room temperature, but we did not clearly observe scrambling or exchange that was rapid on the NMR (chemical shift) time scale. This shows that **1** is stable on the zeolite at a temperature only 25−50 K below those used in the double-pulse experiments. Cation **1** is not the reversible oligomerization product of unrelated species trapped or condensed in the zeolite pores during the thermal quench.

We also designed a more direct experiment to control against the possibility that **1** is formed by quenching other active species of unrelated structure (e.g., simple olefins). We carried out a double-pulse experiment similar to that in Figure 5b with the

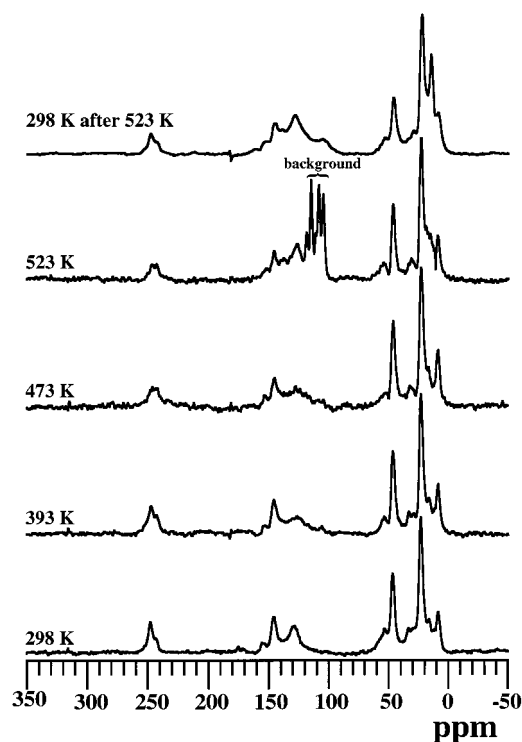(43) Xu, T.; Haw, J. F. *Top. Catal.* **1997**, *4*, 109−118.

Synthesis of Hydrocarbons

J. Am. Chem. Soc., Vol. 122, No. 19, 2000 4769

Figure 7. Variable-temperature ^{13}C MAS NMR study of **1** on zeolite HZSM-5. A single sample was prepared by pulsing ethylene-$^{13}C_2$ onto a catalyst sample at 623 K in a pulse-quench reactor and allowing it to react for 0.5 s. All spectra (Bloch decays) were measured at the temperatures indicated on the figure. ^{13}C signals from Kel-F end caps sealing the MAS rotor are seen in the spectrum measured at 523 K. Cation **1** is present on the catalyst at temperatures approaching those used in the pulse-quench experiments.

following difference. After pulsing ethylene onto the catalyst and allowing it to react at a nominal temperature of 548 K for 60 s, we rapidly quenched the catalyst to 298 K and held it near room temperature in the flow reactor for 300 s. Had we measured the NMR spectrum at this point we would have observed that **1** and related cations accounted for nearly all of the organic species in the catalyst bed. Instead, we rapidly raised the reactor temperature back to 548 K, held it there for 60 s, and then injected a pulse of dimethyl ether. As in the experiment described in Figure 5b, the GC trace showed hydrocarbon synthesis without an induction period. *The thermal quench does not eliminate the catalytic effect.*

Trapping studies were performed to identify the volatile products that exit the catalyst bed during the decomposition of **1** in flow reactors. We achieved this by adding a second zeolite bed downstream of the catalyst bed. The trapping bed contained inactive NaY zeolite pellets, and it was cooled externally with liquid nitrogen to promote condensation of organic species. **1** was generated by pulsing ethylene onto HZSM-5 pellets at 548 K; the gases that immediately exited the reactor were vented to avoid collection of products unrelated to the decomposition of **1**, but between 10 min and 1 h following injection the effluent from the reactor was flowed through the trapping bed. ^{13}C NMR spectra of the NaY pellets were then measured at room temperature; representative results are presented in the Supporting Information, Figure S5. Those experiments showed that the decomposition products of **1** that exit the reactor are propene, toluene, and a smaller quantity of ethylene. Note that this implies that some fraction of the olefins that form cation **1** do so reversibly, although stoichiometry precludes complete reversibility.

Table 1. Theoretical and Experimental ^{13}C Isotropic Chemical Shifts for Cations **1** and **4**[a]

	cation **1**		cation **4**	
	exptl	GIAO-MP2	exptl	GIAO-MP2
C1−C3	250	255.3	245	249.3
C2	148	152.8	155	163.1
C4−C5	48	53.0	43	50.4
methyl (C1−C3)	24	28.9	22	26.7
methyl (C2)			10	12.4

[a] Theoretical values calculated at the GIAO-MP2/tzp/dz level of theory using MP2/6-311+G* geometries and referenced to the ^{13}C chemical shift in TMS (199.0 ppm) calculated at the same level of theory.

Aromatic Compounds as MTO Cocatalysts. Other workers have previously reported that co-feeding toluene or other aromatic compounds enhances the conversion of methanol to hydrocarbons on zeolite HZSM-5.[26,27] We considered the possibility that other cyclic species (clearly distinct from **1**) derived from aromatic compounds could also function as organic reaction centers in MTO chemistry. This proved to be the case. Experiments similar to those described here confirmed that co-injection of large amounts of toluene accelerated the conversion of methanol to hydrocarbons and also formed the pentamethylbenzenium cation **5**. Calculations suggest (vide infra) that

5
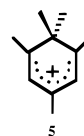
methylation of toluene has a higher barrier than for some of the species related to **1**, and we defer detailed discussion of the conditions under which aromatic species might act to a later report (but see ref 30 for related experiments). In brief, we suspect that a pattern of alkylation and olefin elimination reactions, very similar to those described below for cyclopentenyl species, also operates on aromatic species, once they form at higher temperatures.

Theoretical Results

^{13}C NMR Chemical Shifts of Cations 1 and 4. We optimized the geometries of cations **1** and **4** at the MP2/6-311+G* level; Cartesian coordinates for these are given in the Supporting Information. The C_{2v} symmetry and bond lengths obtained for cation **1** reflect the electron delocalization and partial double bond character expected for this allylic cation. Cation **4** exhibits similar characteristics. The lowest energy geometry of **4** has C_1 symmetry due to methyl group rotations. To decrease the computational cost of the GIAO-MP2 chemical calculations, we obtained an optimized geometry for **4** in which the molecule was constrained to C_s symmetry. The energy difference between the two conformers is negligible.

We report the GIAO-MP2/tzp/dz values of the isotropic ^{13}C chemical shifts for cations **1** and **4** in Table 1. The predicted chemical shift for C1 and C3 in **1** is 255.3 ppm, which compares to the experimental value of 250 ppm. For C2, theory predicts a chemical shift of 152.8 ppm, whereas the experimental value is 148 ppm. The CH_2 carbons are predicted to have isotropic chemical shifts of 50.0 ppm which compare to the measured values of 48 ppm. Finally, the methyl carbons have theoretical values of 28.9 ppm, whereas the experimental chemical shifts are 24 ppm. In all cases the theoretical values are downfield of the experimental chemical shifts, in the worst case by ~5 ppm.
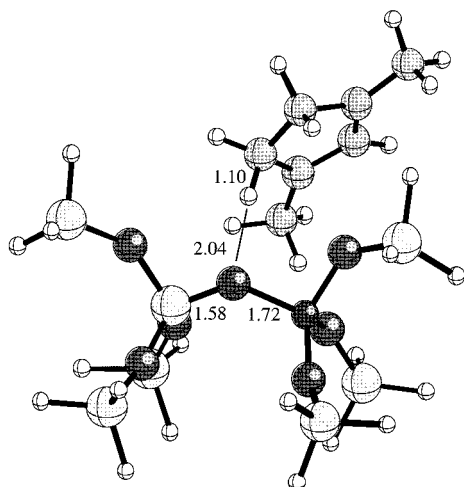
Figure 8. B3LYP/6-311G** optimized geometry of the 1,3-dimethyl-cyclopentadienyl cation **1** coordinated to the zeolite anion (ion-pair structure). The binding energy for the complex is −80.7 kcal/mol.

It is likely that the presence of the conjugate base of the zeolite and motional averaging has some effect on the chemical shifts. Indeed, a notable change in the geometry of the cation is observed theoretically (see below) when it is complexed with a model of the zeolite anion. Although the agreement is less exact than we would like, it is sufficient to verify the presence of **1** within the zeolite.

Similar agreement between theory and experiment was obtained for cation **4**. The distinctive experimental ^{13}C shift for C2 of cation **4**, 155 ppm (see Figure 3), compares with the theoretical value of 163 ppm. The theoretical values for C1 and C3, 249.3 ppm, are also downfield of the 245 ppm experimental value assigned from Figure 3. Other signals in the experimental spectra are good matches for the remaining theoretical shifts if the theoretical values are assumed to be ca. 5 ppm downfield of experiment, as for cation **1**.

Stability of 1 and Related Species on a Zeolite Cluster Model. We have reported that only in rare cases do carbenium ions exist as persistent species in zeolites (under typical conditions of temperature and loading).[44] Whereas we are claiming in this paper that **1** can persist in the zeolite catalyst HZSM-5, it is also important to see if a reasonable theoretical treatment of the system also predicts that **1** is stable *in the presence of the zeolite conjugate base.* In Figure 8 we show the B3LYP/6-311G** optimized geometry of **1** on a cluster model of HZSM-5. The most acidic proton of **1** is in close proximity (2.04 Å) of the zeolite lattice, and could be considered to be involved in a hydrogen bond with the negatively charged zeolite oxygen. The O−H−C angle is 161.2°. The C−H distance for the proton interacting with the oxygen is 0.008 Å longer than the other C−H methylene bonds. Note that the molecule exhibits distortions from that of the free cation. In particular, the C1−C2 (1.375 Å) and C2−C3 (1.405 Å) bond distances, which are equal in the free cation, are different in the complex. Similarly the C1−C5 and C3−C4 distances differ by 0.013 Å and the bonds to the methyl groups differ by 0.027 Å. The total Mulliken charge on the cation is 0.84 |e|.

Although there are certainly many other possible ways the cation could orient itself with regard to the zeolite, this optimization demonstrates that cation **1** is stable over the zeolite anion in the most likely geometry that would promote proton transfer back to the zeolite. The geometry of the complex also supports the indication from the NMR calculation that the lattice has a measurable effect on the cation. Considering the asym-

metry imposed on the cation in the complex, we must assume that motional averaging is sufficient to retain the appearance of C_{2v} symmetry in the experimental NMR spectra.

It is important to consider the energetics involved in the formation of **1** in the zeolite (all values reported are ΔE's). Cation **1** could be formed in principle by the protonation of the parent olefin **2**. The protonation energy of **2** is −229.4 kcal/mol at the B3LYP/6-311G** level. This large exothermic contribution to the reaction energy is countered by the energy needed to remove the proton from the zeolite. At the B3LYP/6-311G* level of theory the deprotonation energy of our zeolite model is 303.2 kcal/mol. If we just consider these two aspects of the reaction, the overall reaction would be endothermic by ≈74 kcal/mol, and thus would be very unlikely to occur. However, upon protonation of the parent olefin and formation of **1**, we also gain the energy of the Coulomb attraction between **1** and the conjugate base of the zeolite. The interaction energy of the ion pair is not insignificant; the Coulomb attraction for two point charges separated by 3 Å is ca. 100 kcal/mol. Indeed, the calculated difference in energy between the ion pair complex and the sum of the energies of the ions at infinite separation is −80.7 kcal/mol.[45] Summing the energy contributions (303.2 − 229.4 − 80.7) we arrive at an overall reaction energy of −6.9 kcal/mol. For comparison, the energy difference between the ion pair complex and the isolated parent olefin and protonated zeolite model is also −6.9 kcal/mol. This result further validates the decomposition of the overall reaction energy into the three contributions cited above. Thus, the large endothermic energy contribution due to deprotonation of the zeolite is balanced by the large exothermic contributions from the basicity of the parent olefin and the ion-pair interaction, leading to a reaction that is overall slightly exothermic.

We have previously found the basicity of parent olefins to be a good predictor of the existence of stable carbenium ions in zeolites.[44] In the prior work, theoretical calculations (MP4-(sdtq)/6-311+G*) suggested that a basicity of 209 kcal/mol or more was required for a stable carbenium ion to form. Those results are consistent with the basicity of the parent olefin of **1** and the observation of **1** as a stable cation in the zeolite.

In previous studies of propene on acidic zeolites, we did not find any evidence for a stable isopropyl carbenium ion on the zeolite. However, experiment and theory were in agreement[46] about the existence of two other states: a π complex of the olefin on the acidic hydrogen[47] and a framework bound isopropoxy species of a type originally proposed by Kazansky.[48] We considered the possibility that a π complex and a framework alkoxy might also be stable states. This proved to be the case. Figure 9 is the B3LYP/6-311G** optimized geometry of the π complex of cyclic diene **2** on a cluster model of HZSM-5. The distance between the acidic proton and the nearest carbon is 2.20 Å and the O−H−C angle is 167.9°. The total Mulliken charge on the olefin is 0.02 |e|. The binding energy for the complex is −4.7 kcal/mol. The electronic energy of the π complex at this level of theory is only 2.2 kcal/mol higher than that of the ion-pair structure in Figure 8. As such, the π complex could plausibly exist in low concentrations on the zeolite.

(44) Nicholas, J. B.; Haw, J. F. *J. Am. Chem. Soc.* **1998**, *120*, 11804−11805.

(45) In this case we are considering the difference in energy between the optimized ion-pair complex and the sum of the energies of **1** and the zeolite conjugate base, both of which were optimized in isolation at the B3LYP/6-311G** level of theory.

(46) Nicholas, J. B.; Xu, T.; Haw, J. F. *Top. Catal.* **1998**, *6*, 141−149.

(47) White, J. L.; Beck, L. W.; Haw, J. F. *J. Am. Chem. Soc.* **1992**, *114*, 6182−6189.

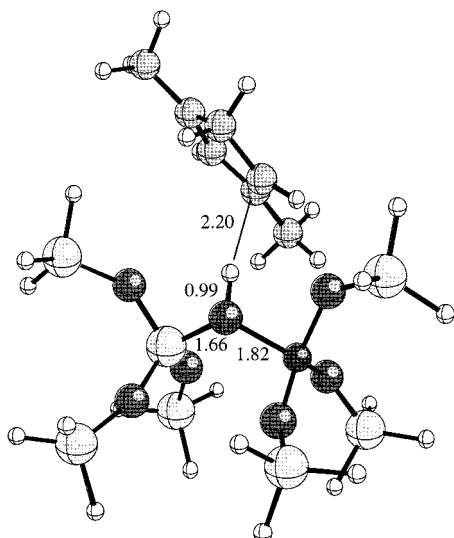(48) Kazansky, V. B. *Acc. Chem. Res.* **1991**, *24*, 379−382.

Figure 9. B3LYP/6-311G** optimized geometry of the π complex formed by adsorbing neutral cyclic diene **2** to the zeolite acid site model used to obtain the ion-pair structure in Figure 8.
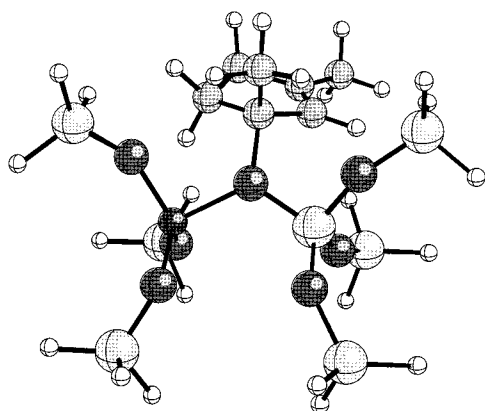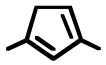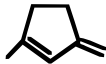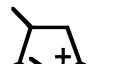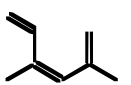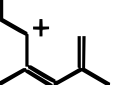

Figure 10. B3LYP/6-311G** optimized geometry of the framework-bound alkoxy species that could form as an alternative to cation **1** (cf., the ion-pair structure in Figure 8).

Figure 10 reports the B3LYP/6-311G** optimized geometry of a framework alkoxy species that was obtained as a stable state when a structure similar to the ion pair was optimized from an initial geometry with a close contact between one of the charged carbons of the cation and a basic oxygen on the zeolite cluster. The energy of the alkoxy complex is 28.4 kcal/mol higher than that of the ion pair. Thus, even if the kinetics were such that the alkoxy could form (we did not make any attempt at determining the barrier to the formation of the alkoxy from the ion pair or from the parent olefin and the protonated zeolite) at equilibrium, the concentration of the alkoxy species would be effectively zero, even at the highest temperatures used in MTG chemistry. We can thus theoretically rule out any involvement of this alkoxy species in the observed chemistry.

Modeling the Roles of 1 in Hydrocarbon Synthesis. The experimental evidence reported above suggests three pathways from **1** to volatile hydrocarbon products. (1) Formation of **1** and related species, including aromatics, from ethylene ends the induction period and opens lower barrier pathways from DME to propene and other olefins. (2) At higher temperatures and while hydride acceptors are present on the catalyst, **1** is an intermediate in the formation of toluene. (3) At longer reaction times, after other products have exited the reactor, cation **1** slowly decomposes on the catalyst to yield toluene and propene.

Table 2. Theoretical (B3LYP/6-311G*) Barriers for Various Methylation Reactions in the Gas Phase

reactants	products	$\Delta E^{\ddagger}$ (kcal/mol)
Ethylene TMO$^+$	Propene DMEH$^+$	48.9
Propene TMO$^+$	1-Butene DMEH$^+$	45.3
Toluene TMO$^+$	*p*-Xylene DMEH$^+$	41.6
[cyclic diene] TMO$^+$ DME+ CH$_3$OH$_2$+	[cyclopentenyl cation]$^+$ DME CH$_3$OH H$_2$O	32.9 63.5 62.9
[methylene cyclopentene]	[cyclopentenyl cation]$^+$ DME	34.6
[cyclopentenyl cation]$^+$ DME CH$_3$OH	[methyl cyclopentenyl cation]$^+$ CH$_3$OH H$_2$O	63.5 62.9
[triene] TMO$^+$	[allyl cation]$^+$ DME	40.3

We modeled parts of the first two pathways using theoretical chemistry.

In the traditional view of MTG/MTO chemistry, ethylene forms from DME by some means and then propene is formed by methylation of ethylene. Further methylation steps lead to successively higher olefins. As a step to understanding how the formation of cation **1** in the zeolite accelerates DME conversion, we used theoretical methods to calculate the reaction pathways for methylation of various organic species present or assumed to be present under reaction conditions. Theoretical (B3LYP/6-311G*) calculations of the reactants, products, and transition states were carried out for each of the reactions in Table 2. In each case we calculated the reaction path (using the intrinsic reaction coordinate procedure[49] in Gaussian98) to ensure that that the transition state linked the reactant and product states. The hydrocarbon reactants included ethylene, propene, toluene, the cyclic diene **2**, and other olefins related to cation **1**. Consideration of **2** is justified by the low energy difference between the π complex of **2** on the zeolite and the ion-pair complex of **1** and the anion site (cf., Figures 8 and 9).

In modeling the methylation of neutral hydrocarbon reactants, we had several choices for the methylating agent. CH$_3{}^+$ is not a plausible intermediate by itself, although CH$_3{}^+$ groups bound to the conjugate base sites (so-called "surface methoxys") might be able to act as methylating agents. We do not observe any such groups under our experimental conditions. The low proton affinity of methanol (exptl 180.3 kcal/mol) argues against CH$_3$-

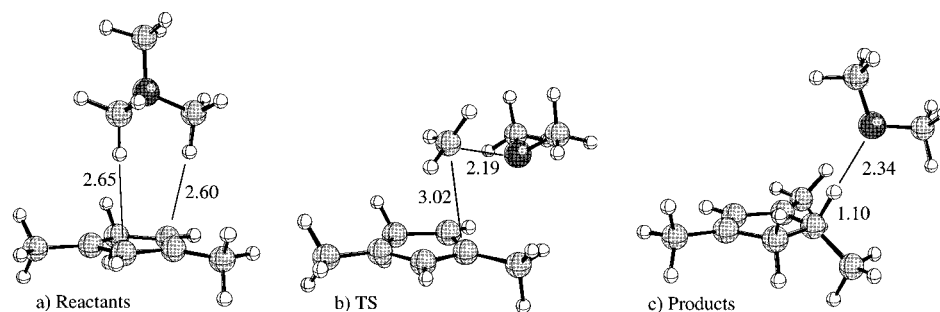(49) Gonzalez, C.; Schlegel, H. B. *J. Chem. Phys.* **1989**, *90*, 2154−2161.

Figure 11. B3LYP/6-311G* optimized geometries of the three stable points along the reaction pathway for the conversion of trimethyloxonium cation and cyclic diene **2** to DME and cation **3**: (a) reactants (0 kcal/mol); (b) transition state (+32.9 kcal/mol); and (c) products (−35.1 kcal/mol).

OH_2^+ existing in the zeolite as a stable species. Dimethyl ether is more basic (exptl 189 kcal/mol), and thus protonated dimethyl ether, $(CH_3)_2OH^+$ (DMEH$^+$), would be a more likely to have an appreciable lifetime in the zeolite. An even more stable species is the trimethyloxonium cation, TMO$^+$. At room temperature and slightly above, this cation has been observed in the zeolite by NMR in the presence of an excess of ether.[50−52] Furthermore, several of the classical mechanisms of MTG chemistry are formulated using TMO$^+$. Running counter to the indications of methylation agent stability is the energy required for methyl group donation. Thus, while $CH_3OH_2^+$ dissociation into CH_3^+ and H_2O is uphill by 79.4 kcal/mol (ΔE at B3LYP/6-311G*), it is 88.8 kcal/mol endothermic for DMEH$^+$ to donate a CH_3^+ group, while methyl donation by TMO$^+$ is uphill by 99.3 kcal/mol. For the reaction of TMO$^+$ and ethylene, the initial products obtained are $CH_3-CH_2-CH_2^+$ and DME. However, the relative proton affinities of these molecules are such that a proton is further transferred during the optimization, giving as final products propene and DMEH$^+$. The overall reaction is exothermic by 15.1 kcal/mol and the barrier is 48.9 kcal/mol. Similarly, the reaction of TMO$^+$ and propene passes through a barrier of 45.3 kcal/mol to initially form $CH_3-CH^+-CH_2-CH_3$ and DME, followed by proton transfer to form 1-butene and DMEH$^+$. The overall reaction is exothermic by 10.7 kcal/mol. The barrier for methylation of toluene to form *p*-xylene, 41.6 kcal/mol, is also fairly high. Figure 11 reports the structures of the stable states on the pathway for the reaction of TMO$^+$ with cyclic diene **2**. In contrast to the reactions of the simple olefins or toluene, the products obtained with **2** were DME and a carbenium ion, **3**. This reaction is also exothermic, by 35.1 kcal/mol, but the reaction barrier is significantly lower than that for the simple olefins, 32.9 kcal/mol. Methylation of **2** by either $CH_3OH_2^+$ or DMEH$^+$ involves much higher energy barriers (62.9 and 63.5 kcal/mol). Thus, the lower energy requirements for CH_3^+ dissociation by these species (versus TMO$^+$) do not result in more favorable energy barriers for methyl donation to **2**. A low barrier was also obtained for an isomer of **2** with an exo-cyclic double bond (34.6 kcal/mol). In the gas phase, the calculated energy of *exo*-**2** is only 1.1 kcal/mol above that of the endo isomer. We also considered the possibility that the cyclic dienes could ring-open to open-chain species, and these could be active species in methylation reactions. Table 2 reports results that the barrier for methylating an open-chain triene related to cation **3** is 40.3 kcal/mol. However, formation of the triene from the cyclic diene is endothermic by 17.7 kcal/mol. Thus, the effective barrier for this route is also high.

We also considered the possibility that cations **1** or **3** undergo direct methylation (i.e., without prior deprotonation) by either DME or methanol. The transition states for the reactions reported in Table 2 involve a concerted exchange of H$^+$ for CH_3^+. In effect, in the transition state H$^+$ must be substantially removed from the cations prior to methylation. Not surprisingly, the barriers for these direct methylation reactions are quite high. In summary, the calculations reported in Table 2 suggest that cyclic dienes, in equilibrium with cyclopentenyl cations under reaction conditions, provide a pathway for carbon−carbon bond formation with a lower barrier than for other species likely to be present in the catalyst.

We studied the mechanism by which cation **1** can form toluene under reaction conditions. Skeletal rearrangement reactions are invariably complex and involve a number of bond making and breaking steps; nevertheless, they are characteristic of organic chemistry in liquid and solid acids. Here we simply consider reactions in the gas phase and do not attempt to model the hydride accepting species or the zeolite. The reaction stoichiometry for producing a C_7H_8 species from $C_7H_{11}^+$ implies that there must be a means by which H_2 and H$^+$ are lost. There is no apparent mechanism by which H_2 can be lost directly, therefore the reaction must involve the loss of H$^-$ and two H$^+$ in three separate steps. The following is a speculative mechanism, based entirely on theoretical predictions. In several cases the proposed mechanism involves molecules that can exist as two or three different isomers. In each case we assume that only the lowest energy isomer is involved.

Each species in Figure 12 was optimized at MP2/6-311+G*, but we focus only on the relative electronic energy of each species and do not detail the geometries obtained. Cation **1** can lose H$^+$ to form the parent olefin **2**, as discussed above. There are two other configurational isomers of this species that vary by the positions of the methyl groups on the ring. The lowest energy isomer is **2a**. Isomer **2b** is only 0.5 kcal/mol higher in energy, and thus is very likely to be present in the zeolite during the course of the reaction. Protonation of either of these two isomers gives **1**. The other isomer (**2c**) is 3.6 kcal/mol higher in energy, and is thus less likely to be formed. Isomer **2c** also does not give **1** upon protonation. We will only consider **2a** in subsequent steps of the reaction. We have earlier shown that the protonation energy of **2a** is 228.6 kcal/mol at the B3LYP/6-311G* level of theory. At the MP2/6-311+G* level of theory used for the calculation of the reaction path, the protonation energy is reduced to 217.9 kcal/mol.

Isomer **2a** can lose H$^-$ to any cation equivalent present (e.g., an alkoxy species derived from propene) to form the $C_7H_9^+$ species **6a**. Loss of H$^-$ is highly endothermic (270.1 kcal/mol at MP2/6-311+G*) and thus must be countered by a similarly large exothermic contribution from the binding of H$^-$ to some

(50) Haw, J. F.; Xu, T.; Nicholas, J. B.; Goguen, P. W. *Nature* **1997**, *398*, 832−835.
(51) Munson, E. J.; Kheir, A. A.; Haw, J. F. *J. Phys. Chem.* **1993**, *97*, 7321−7327.
(52) Munson, E. J.; Haw, J. F. *J. Am. Chem. Soc.* **1991**, *113*, 6303−6305.
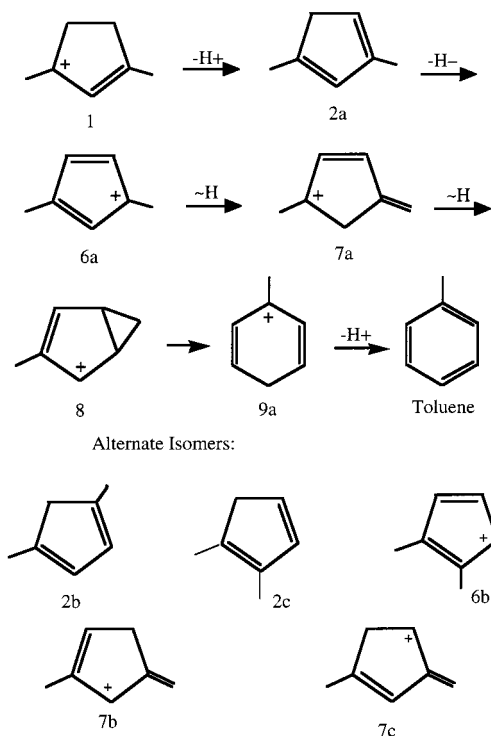
Figure 12. Proposed reaction mechanism for the conversion of **1** to toluene. While this is shown in schematic form, each structure shown (as well as all reasonable isomers thereof) was optimized at the MP2/6-311+G* level.

other cation or incipient cation. Another isomer (**6b**) is 7.6 kcal/mol higher in energy.

Cation **6a** can then undergo a hydride shift, to form a species with an exocyclic double bond (Figure 12). There are three such $C_7H_9^+$ isomers. The lowest energy isomer predicted by the MP2/6-311+G* level of theory is **7a**. Isomer **7b** is 4.3 kcal/mol higher in energy. The third isomer (**7c**) is much less stable, being 21.1 kcal/mol higher in energy than **1**. Formation of **7a** from **6a** is predicted to be exothermic by 22.0 kcal/mol. We again assume that the reaction involves only isomer **7a**.

Isomer **7a** can then undergo an additional hydride shift, which results in the formation of **8** (Figure 12). Molecule **8** is 13.6 kcal/mol higher in energy than **7a**. This destabilization is due in large part to the change from a tertiary carbenium ion (**7a**) to a secondary carbenium ion (**8**), although **8** is an allyl as well as a cyclopropylcarbinyl cation. The formation of the three-membered ring also imparts strain, and thus a higher energy state.

However, from **8** the ring can open to form the toluenium cation. The ring opening of **8** naturally produces the para isomer of the toluenium cation (**9a**). At the MP2/6-311+G* level, this step is predicted to be 20.9 kcal/mol exothermic. There are obviously three isomers of the toluenium cation. As expected, the para isomer is lowest in energy. The ortho isomer is 1.3 kcal/mol higher in energy, whereas the meta isomer is 4.3 kcal/mol less stable than the para cation. We assume that the reaction proceeds via the para isomer.

In the final step of the reaction **9a** would lose H^+, possibly by donation to a deprotonated acid site, and generate toluene (Figure 12). The calculated protonation energy of toluene is 185.8 kcal/mol. We previously stated that a basicity of ≈209 kcal/mol is required of the parent olefin or aromatic for a long-lived carbenium ion to form.[44] Thus, we would assume that the toluenium cation is not stable in the zeolite, and readily forms toluene.

Discussion

Formation and Decomposition of Cyclopentenyl Cations. Signals due to carbenium ion **4** were observed in an early NMR study of products formed when propene was exposed to zeolite HY at room temperature,[53] and this assignment was established in 1989.[42] Cations **1**, **4**, and similar cations with other substituents have since been observed by NMR in studies of various olefins and alcohols on acidic zeolites.[54,55] Alkyl-substituted cyclopentenyl cations are indefinitely stable in zeolites at room temperature; as such they join the trityl,[56] indanyl,[57] and pentamethylbenzenium[30] cations in a small group of persistent cation classes characterized in zeolites by NMR. Cyclopentenyl cations have also been detected on zeolites and other solid acids using UV spectroscopy.[58] The observation here that theory correctly predicts the stability of the ion-pair structure of **1** on the zeolite anion site (Figure 8) is a satisfying result.

We have not fully identified the mechanism by which ethylene forms cation **1** in the zeolite, but Figure 3 shows that oligomerization occurs at low temperatures and cation **1** is present even at 373 K. Stoichiometry dictates that the formation of **1** from ethylene also requires formation of alkanes. For example, consider a reaction where the only products are **1** and propane:

$$13C_2H_4 + 2ZeoOH \rightarrow 2C_7H_{11}^+ + 2ZeoO^- + 4C_3H_8$$

where ZeoOH denotes a zeolite Brønsted site and ZeoO$^-$ the conjugate base of such a site. Analogous schemes may be written for other alkane coproducts, and indeed we observe light alkanes in the volatile products following the injection of ethylene. In the double-pulse experiments described above, the ethylene that formed cation **1** was delivered in the first pulse. Without an olefin pre-pulse, the conversion of methanol or DME exhibits an induction period (cf., Figure 1). An unknown, but inefficient mechanism of olefin synthesis operates during the induction period and accumulation of oligomeric species in the zeolite leads to **1.** We have not here attempted to identify the mechanism of the induction reaction, but we sometimes detect small quantities of ethylene during the induction period, which is consistent with most mechanisms for the formation of the "first" carbon–carbon bond.

Balanced chemical reactions (albeit with large coefficients) can be written that are consistent with the observed decomposition products of **1** at long reaction times. For example:

$$9C_7H_{11}^+ + 9ZeoO^- \rightarrow 6C_7H_8 + 7C_3H_6 + 9ZeoOH$$

This balanced reaction predicts that **1** decomposes to yield roughly equal amounts of propene and toluene, as is observed. Similar balanced reactions can account stoichiometrically for the ethylene that is observed. Unimolecular decomposition of **1** would form products that we do not observe, such as acetylene and cylopentene or ethylene (observed) and cyclopentadiene. A more plausible mechanism for the decomposition of **1** is deprotonation of **1** to form **2** (calculated to be uphill by only ca. 2 kcal/mol) which then diffuses in the zeolite until it encounters a second **1**. Intramolecular hydride transfer (dispro-

(53) Zardkoohi, M.; Haw, J. F.; Lunsford, J. H. *J. Am. Chem. Soc.* **1987**, *109*, 5278–5280.
(54) Xu, T.; Haw, J. F. *J. Am. Chem. Soc.* **1994**, *116*, 7753–7759.
(55) Stepanov, A. G.; Vladimir, N. S.; Zamarev, K. I. *Chem. Eur. J.* **1996**, *2*, 157–167.
(56) Tao, T.; Maciel, G. E. *J. Am. Chem. Soc.* **1995**, *117*, 12889–12890.
(57) Xu, T.; Haw, J. F. *J. Am. Chem. Soc.* **1994**, *116*, 10188–10195.
(58) Sommer, J.; Sassi, A.; Hachoumy, M.; Jost, R.; Karlsson, A.; Ahlberg, P. *J. Catal.* **1997**, *171*, 391–397.

portionation) between **1** and **2** would then form toluene and a cyclic olefin that would further react on the catalyst. An inefficient decomposition mechanism is consistent with the long half-life of cation **1** in the absence of other reactants which can act as hydride acceptors and open a more direct pathway to toluene (Figure 12).

Earlier work has speculated on roles for cyclopentenyl cations in the synthesis of aromatics.[54,58,59] The experimental demonstration of the intermediacy of **1** in the synthesis of toluene is an important feature of the present study. In the design of MTO processes, it is desirable to form olefins while minimizing aromatics. Ironically, on zeolite HZSM-5 cation **1** promotes the formation of olefins, but it is also an intermediate in the pathway to aromatics. A C_7 carbenium ion is the precursor to the C_7 aromatic product. We also observe cations with substitution patterns similar to **4** and speculate that some of the xylene products form directly from this more highly substituted C_8 carbenium ion.

How Could Cyclopentenyl Cations Catalyze Propene Synthesis? Immediately following the induction period, we see a very high selectivity for propene, 80+% of the total olefin yield. In particular, we see far more propene than ethylene. The results in Table 2 indicate that methylation of propene to form butene should be even easier than methylation of ethylene to form propene. If, on a working catalyst, the propene is formed from ethylene, why would chain growth stop after a single methylation reaction? Pulsing ethylene onto zeolite HZSM-5 catalyst rapidly synthesizes cation **1** (and related species such as cation **4**) with very high selectivity. Cation **1** also forms naturally from the ethylene obtained when methanol or DME are slowly converted during the induction period. A number of observations in the literature point to roles for cyclopentenyl cations or closely related species in olefin synthesis on acidic zeolites. For example, Langner observed an induction period in the synthesis of hydrocarbons from methanol on NaHY catalyst and found that this was shortened by co-feeding small amounts of other alcohols.[60] Co-feeding ethanol shortened the induction period by a factor of ca. 2, but co-feeding cyclohexanol reduced the induction period by a factor of nearly 20. In our recent communication,[21] we used the pulse-quench reactor to asses the effect of pulsing various compounds on the subsequent conversion of methanol. Pulsing 2-propanol was effective in eliminating the induction period, but an even greater conversion was obtained with a smaller quantity of the cyclic diene **10**, a more direct precursor to cation **1**. Formation of **1** in

10

the catalyst, by any means, is correlated with a dramatic increase in hydrocarbon synthesis. When cation **1** is removed from the zeolite bed by decomposition over time, the catalytic effect is removed and the induction period returns.

The barriers to direct methylation of cations **1** or **4**, reported in Table 2, are quite high. However, if the cations first deprotonate, the methylation barriers for the resulting olefins are significantly lower than for other species in the table. Recall that the theoretical energy for the π complex of olefin **2** on a zeolite is only 2.2 kcal/mol higher than that of cation **1**. Thus, the total barrier for **1** to deprotonate followed by methylation of **2** to form cation **3** is still 10 kcal/mol lower than the barrier

(59) Shulz, H.; Wei, M. *Microporous Mesoporous Mater.* **1999**, *29*, 205−218.

(60) Langner, B. E. *Appl. Catal.* **1982**, *2*, 289−302.

to convert ethylene to propene. Methylation of the exocyclic isomer of **2** directly produces a cyclopentenyl cation with an ethyl substituent, **11**.

11
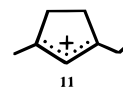
Cation **11** could also form by rearrangement of cation **3**. Like many skeletal rearrangements, the detailed mechanism for converting **3** to **11** requires a number of elementary steps, but the essence of this rearrangement is a $5 \rightleftharpoons 6$ ring expansion−contraction, Scheme 1.

Alkyl-substituted cyclohexenyl cations such as **12** are slightly less stable than cyclopentenyl cations with similar substitution patterns. By similar routes, cation **11** can undergo an additional deprotonation, methylation step to form cation **13**, with a propyl

13
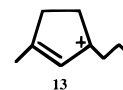
side chain. Skeletal rearrangements as in Scheme 1 are consistent with our earlier observation that propene molecules exiting the reactor contain carbon atoms derived from both the olefin pulse that synthesized **1** and a subsequent methanol pulse.[21]

Cations **11** and **13** can eliminate ethylene and propene, respectively, by hydride migration followed by elimination, as shown for cation **11** in Scheme 2.

In Scheme 2, a primary carbenium ion (or a closely related protonated cyclopropane) is *formally* required as an intermediate in the elimination of ethylene. The analogous *formal* route from **13** to propene requires only a secondary cation intermediate. On this basis alone, a qualitative argument for the propene selectivity could be made based on the relative stabilities of primary and secondary cations. Better yet, we calculated (B3LYP/6-311G*) both reaction pathways, and these are reported in Figure 13. The structures of intermediates and transition states as well as their relative electronic energies are shown for elimination of ethylene, and energies only are shown for the analogous elimination of propene (the structures are very similar). Figure 13 shows that these elimination reactions do not in fact have either primary or secondary carbenium ions as intermediates. The first hydride-transfer step leads to cyclopropane ring closure to form a tertiary cation intermediate, and structures similar to primary or secondary cations are seen only in the transition states, the second of which forms ethylene or propene. Cyclopropylcarbinyl cations, seen in Figures 12 and 13, are well-characterized intermediates in a variety of acid-catalyzed rearrangements in solution.[61,62]

Comparing the energies in Figure 13, one sees that elimination of ethylene by cation **11** involves an overall barrier of 58.3 kcal/mol, but the corresponding barrier is 16.1 kcal/mol lower for elimination of propene by cation **13**. This difference easily accounts for the selectivity of propene over ethylene. Cyclic cations with C_4 or larger alkyl chains would eliminate C_4 or higher olefins as primary products, but if the elimination of propene is rapid at reaction temperature, longer chains would have little opportunity to form. In the zeolite, the intermediates and transition states corresponding to those in Figure 13 would be stabilized by interaction with the framework, but this will not greatly affect the *relative* energetics for producing propene vs ethylene. Note that cyclopentenyl cations are not the only precursors to elimination reactions that account for the olefin selectivity; we would expect to see analogous mechanisms and

Synthesis of Hydrocarbons

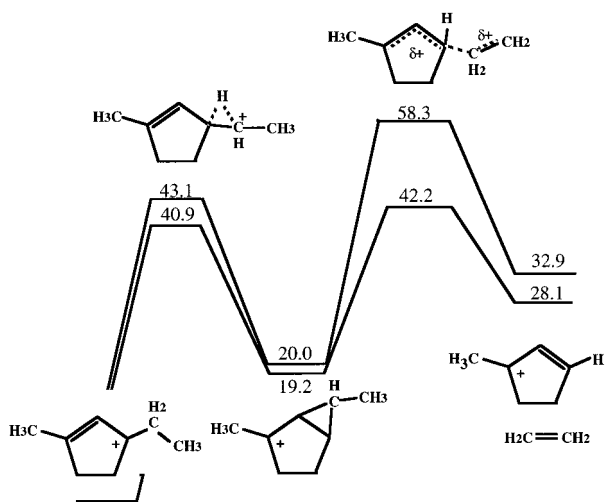*J. Am. Chem. Soc., Vol. 122, No. 19, 2000* 4775

Figure 13. Potential energy surfaces (kcal/mol) for removal of ethylene or propene from cations **11** or **13**, respectively. All minima and transition states were optimized at B3LYP/6-311G*. Schematic structures are shown only for the reactions of **11** to form ethylene; very similar structures were obtained for the analogous pathway to propene. Note that the pathway avoids primary and secondary carbenium ion intermediates (cf. the formal mechanisms in Scheme 2). For each state the relative energy along the ethylene pathway was higher in energy than that of propene.

Scheme 1
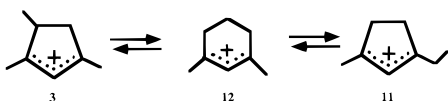
Scheme 2
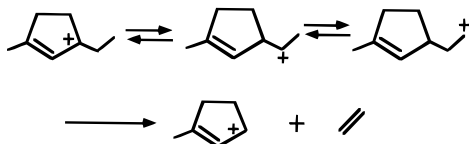
the same selectivity prediction for eliminating olefins from, for example, aromatic rings.

Olefin elimination from cations **11** and **13** also forms a monomethyl cyclopentenyl cation. A closed catalytic cycle is obtained by deprotonation and methylation of this species to reform cation **1**. B3LYP/6-311G** optimizations of the monomethylcation and olefin in contact with the zeolite model (Figures S6 and S7, similar to geometries shown in Figures 8 and 9) indicate that this is possible. In this case, the carbenium ion–zeolite complex is only 0.9 kcal/mol lower in energy than the corresponding olefin complex. Thus the overall reaction, on a working catalyst, converts three methanol molecules to propene and water, and the carbon–carbon bond making and breaking steps occur on cyclic dienes to form cyclopentenyl cations. The proposal advanced here that pentacyclic species are intermediates in the synthesis of olefins suggests parallels to early proposals of the mechanisms of catalytic reforming and bifunctional ring opening.[63–68] The elimination of olefins from polymethylated cyclopentyl cations echoes another early observation that hexamethylbenzene reacts under hydrocracking conditions to form isobutane and xylenes.[69]

Conclusions

The mechanism of MTO/MTG chemistry on zeolite HZSM-5 has several distinct roles for cyclopentenyl cations. These cations form during the induction period from small amounts of olefin formed in an "induction reaction". On zeolite HZSM-5 the principal role of the induction reaction is to synthesize the cyclopentenyl cations that characterize a working catalyst. Once these cations are present, a more efficient mechanism for hydrocarbon synthesis opens up, and the induction reaction takes on a subordinate role. Cyclopentenyl cations are stable species on zeolite acid sites, but the cyclic dienes obtained by their deprotonation are also stable at very slightly higher energies (cf., **1** and **2**). Thus, the cations act as reservoirs of cyclic dienes at reaction temperature and these are much more easily methylated than ethylene or propene. Side chain methylation and skeletal isomerizations lead to cations with alkyl substituents, and these eliminate propene more readily than ethylene. At higher temperatures and conversions, many olefinic and aromatic compounds are present in the catalyst, and some of these may also be methylated and eliminate olefins.

In the presence of hydride acceptors such as olefins, cation **1** is an intermediate in the synthesis of toluene. Thus, a species with a catalytic role in MTO processes is also an intermediate in MTG chemistry, and suppressing aromatic products in MTO on HZSM-5 is necessarily challenging. In the absence of feed, cation **1** slowly decomposes to toluene, propene, and ethylene.

Olefins, aromatics, and other hydrocarbons are, of course, reactive on solid acids, and secondary products are readily observed in MTO/MTG chemistry, especially at higher temperatures or with longer contact times. For example, toluene is methylated to *p*-xylene (Table 2) and propene oligomerizes and cracks to an equilibrium distribution of olefins. These processes are also very interesting and important. The present investigation has focused on primary reactions leading to olefinic (MTO) and aromatic (MTG) products.

Supporting Information Available: Two tables listing atomic coordinates for the species modeled theoretically and eight figures reporting results referred to in the text (PDF). This material is available free of charge via the Internet at http://pubs.acs.org.

(61) Olah, G. A.; Reddy, V. P.; Prakash, G. K. S. *Chem. Rev.* **1992**, *92*, 69−95.
(62) Mayr, H.; Olah, G. A. *J. Am. Chem. Soc.* **1977**, *99*, 510−513.
(63) Sinfelt, J. H.; Rohrer, J. C. *J. Phys. Chem.* **1961**, *65*, 978−981.
(64) Carter, J. L.; Cusumano, J. A.; Sinfelt, J. H. *J. Catal.* **1971**, *20*, 223−229.
(65) Cristoffel, E.; Fetting, F.; Vierrath, H. *J. Catal.* **1975**, *40*, 349−355.
(66) Cristoffel, E.; Röbschläger, K.-H. *Ind. Eng. Chem. Prod. Res. Dev.* **1978**, *17*, 331−334.
(67) Weitkamp, J.; Schulz, H. *J. Catal.* **1973**, *29*, 361−366.
(68) Dautzenberg, F. M.; Platteeuw, J. C. *J. Catal.* **1970**, *19*, 41−48.
(69) Sullivan, R. F.; Egan, C. J.; Langlois, G. E.; Sieg, R. P. *J. Am. Chem. Soc.* **1961**, *83*, 1156−1160.